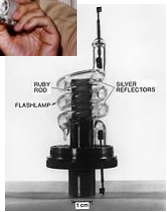
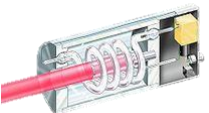
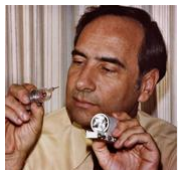


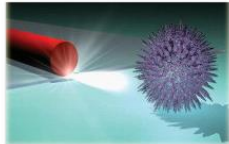
## The ruby laser

Theodore Maiman, 1960



- High speed optical communication and data processing
- On-chip integrated optical circuits
- New perspectives in bio-medical imaging and sensing
- 3D displays and advanced holography
- Ultrafast spectroscopy
- Single molecule detection
- ....

## Nanolasers



# Challenges for nanolasers

- **Limit of diffraction:**

optically mode confinement  $> \lambda/2n$

- Complexity and costs:

Lasing well below damage threshold

Manufacturing expenses

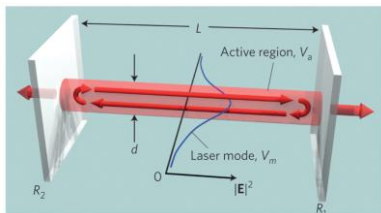
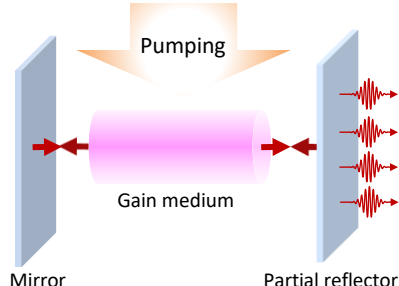
Operating conditions (**room temperature**)

- Large scale integration with silicon-based electronics and light emitting devices

- **Directional emission**

- Simple pumping schemes

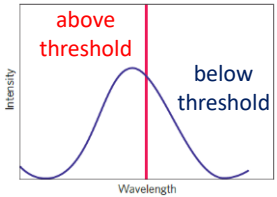
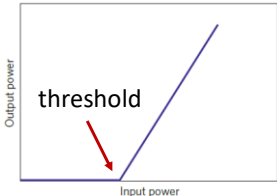
- Proper gain materials to overcome losses



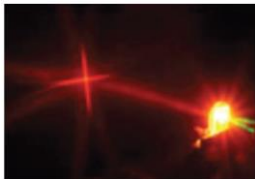
# How to recognize lasing?

Criteria for lasing include:

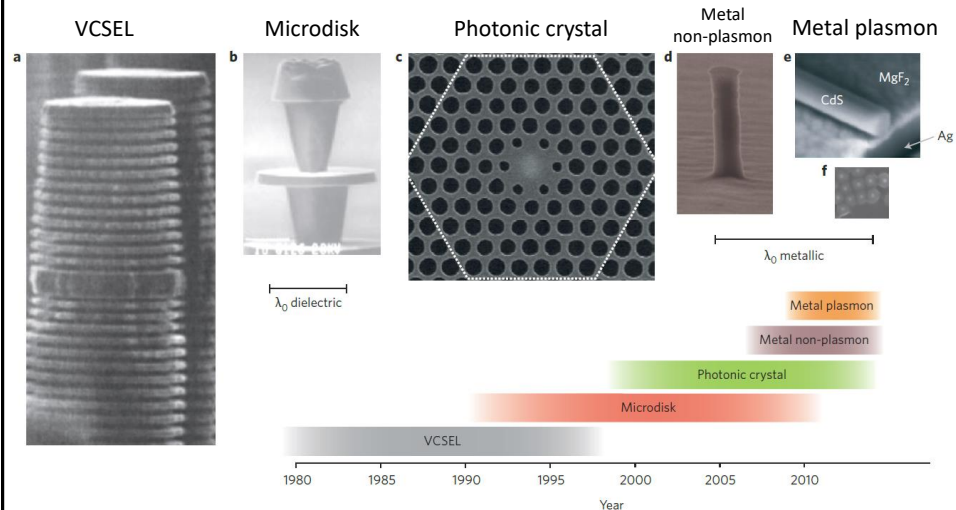
1. A deterministic lasing **threshold** in the input power-output intensity curves.
2. A **steep increase** in the output intensity above threshold.
3. **Linewidth narrowing** above threshold ( $\text{FWHM} < 1 \text{ nm}$ ).
4. **Minor divergence** of the emission beam (directional emission).
5. Spatial and temporal **coherence**.



Competing phenomena, such **amplified spontaneous emission** (ASE) need to be taken into account.

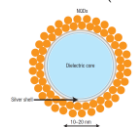


# The race for nanolasers

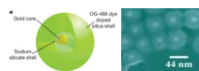


# Plasmonic nanolasers

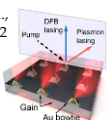
D.J. Bergman & M.I. Stockman,  
PRL 90 027302 (2003)



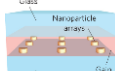
M.A. Noginov et al.,  
Nature 460 1110 (2009)



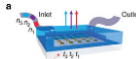
J.Y. Suh et al.,  
Nano Lett. 12 5749 (2012)



W. Zhou et al.,  
Nat. Nanotech. 8 506 (2013)

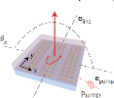


A. Yang et al.,  
Nature Comm. 6 6386 (2015)



T.K. Hakala et al., Nature  
Commun. 10.1038 (2017)

D. Wang et al., Nature  
Nanotech. 10.1038 (2017)

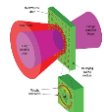


F. Van Beijnum et al.,  
PRL 110 206802 (2013)

Hsin-Yu Wu et al., Adv.  
Optical Mater. 10.1002 (2016)

2003... 2008 2009 2010 2011 2012 2013 2014 2015 2016 2017 2018 2019...

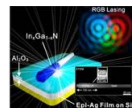
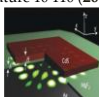
N.I. Zheludev et al.,  
Nat. Photon. 2 351 (2008)



X. Zhang et al.,  
Nature 461 629 (2009)



R.-M. Ma et al.,  
Nature 10 110 (2011)

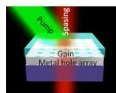


H. T. Rekola et al., ACS  
Photonics 10.1021 (2018)

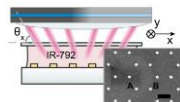
X. Meng et al.,  
Nano Lett. 13 4106 (2013)



Y.-J. Lu et al.,  
Nano Lett. 14 4381 (2014)

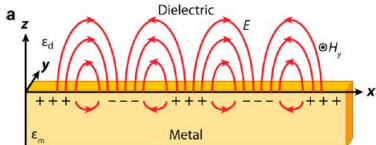


X. Meng et al., Laser Photon.  
Rev. 8 896 (2014)

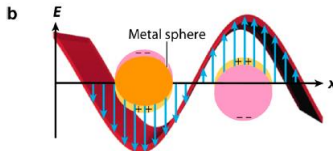


R. Guo et al.,  
PRL 122, 013901 (2019)

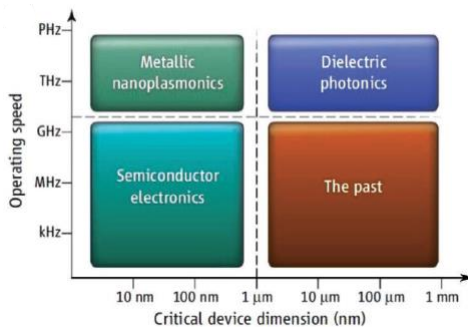
# Surface plasmons in metals



Surface plasmon polariton from a thin metal film



Localized surface plasmons from metal NPs



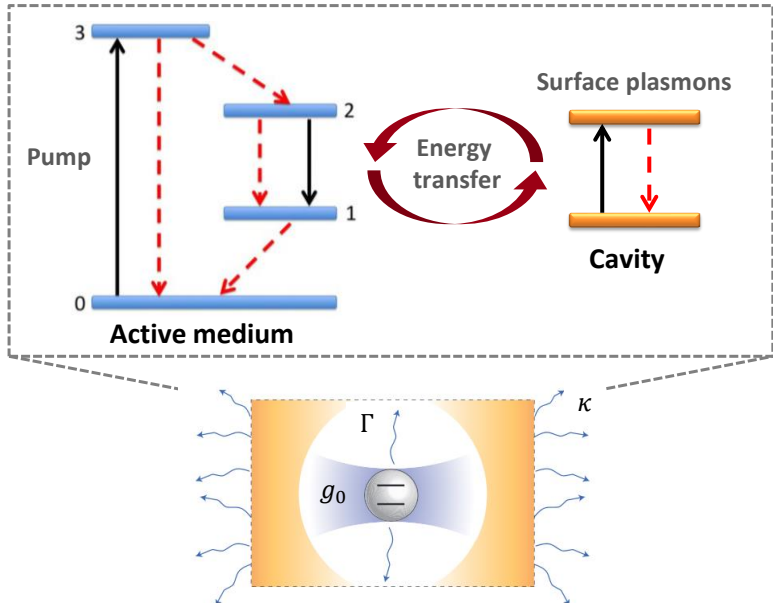
Metal cavities can achieve nanoscale footprints.



High losses (ohmic losses) are introduced.



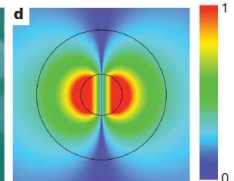
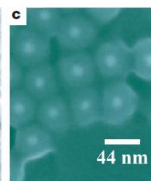
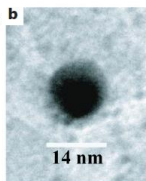
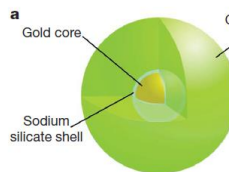
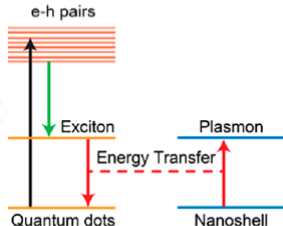
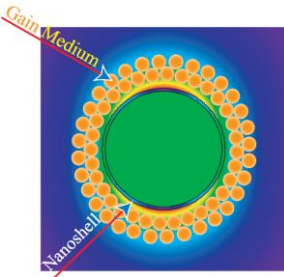
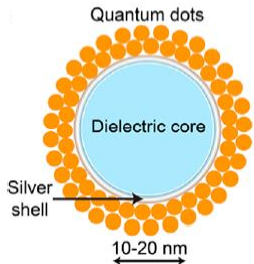
## Plasmonic nanolasers



## SPASER

## Surface Plasmon Amplification by Stimulated Emission of Radiation

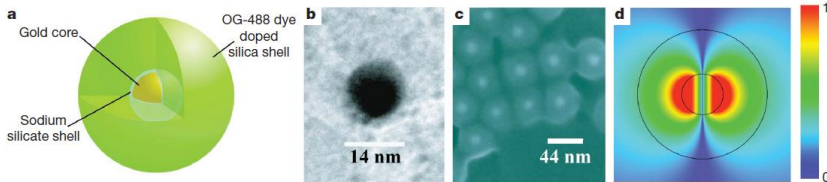
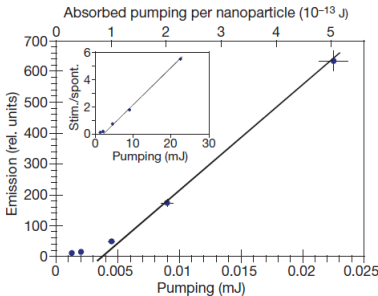
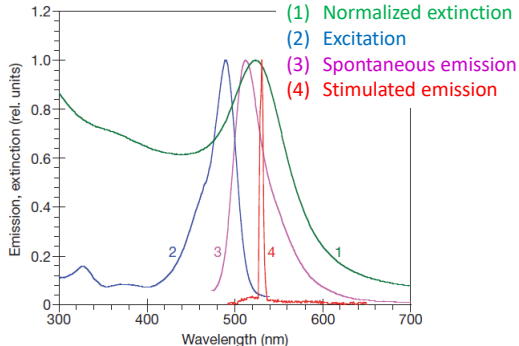
D.J. Bergman &amp; M.I. Stockman, PRL 90 027302 (2003)



M.A. Noginov et al., Nature 460 1110 (2009)

## Demonstration of a spaser-based nanolaser

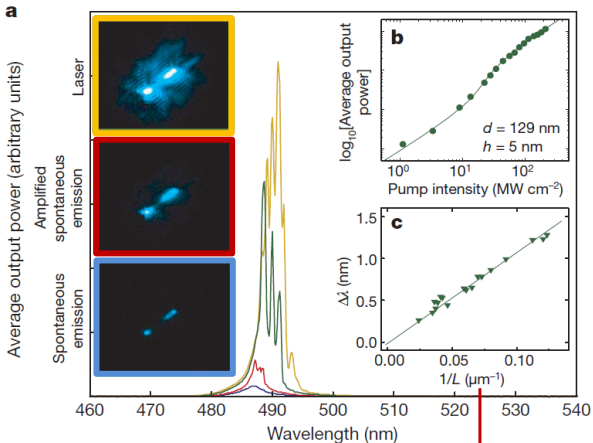
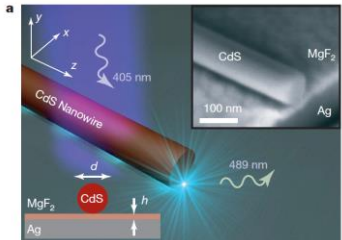
M.A. Noginov et al., Nature 460 1110 (2009)



## Nanowire-on-film laser

## Plasmon laser at deep sub-wavelength scale

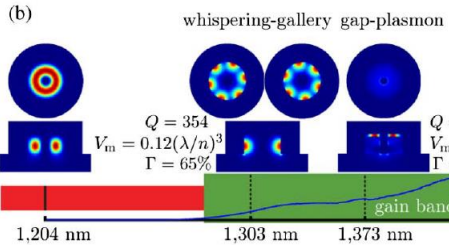
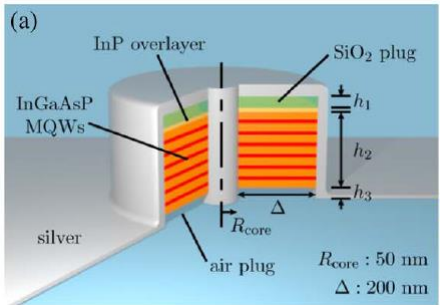
R. F. Oulton et al., Nature 461 629 (2009)



Lack of directional emission in far-field due to scattering at the end facets of the nanowire.

# Metallic nanolasers

W.E. Hayenga et al., Optica. 3 1187 (2016)

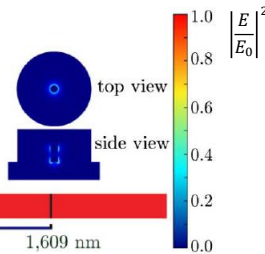


$Q$  = quality factor

$\Gamma$  = extent of energy confinement to the semiconductor region (overlap factor).

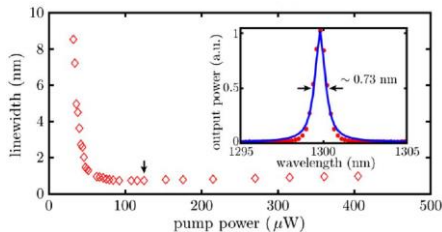
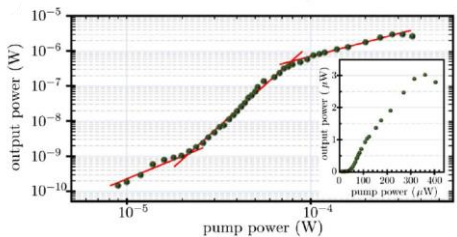
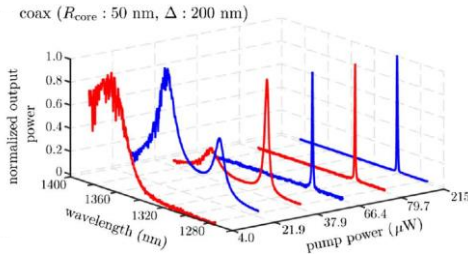
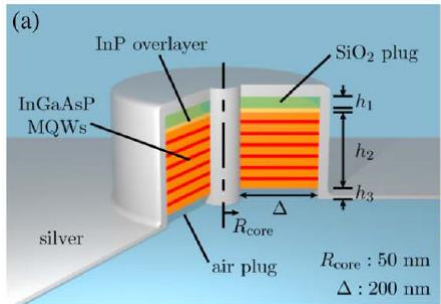
$V_m$  = modal volume

1064 nm fiber laser CW pumping at 77 K



## Metallic nanolasers

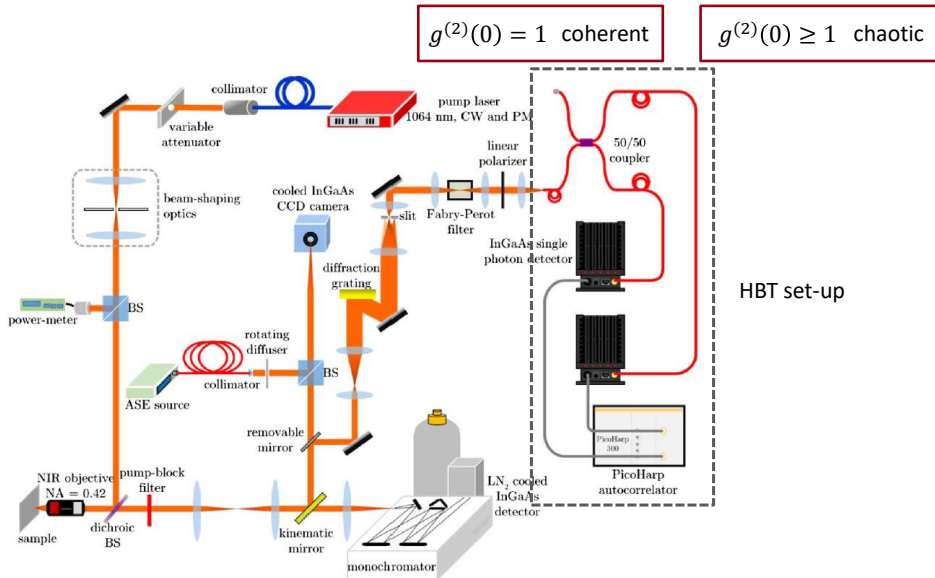
W.E. Hayenga et al., Optica. 3 1187 (2016)



# Metallic nanolasers

## Second-order coherence properties

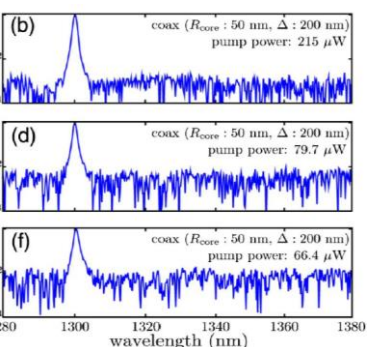
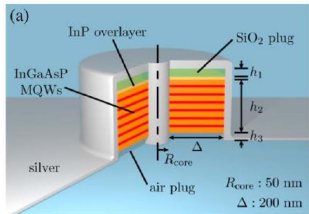
W.E. Hayenga et al., Optica. 3 1187 (2016)



# Metallic nanolasers

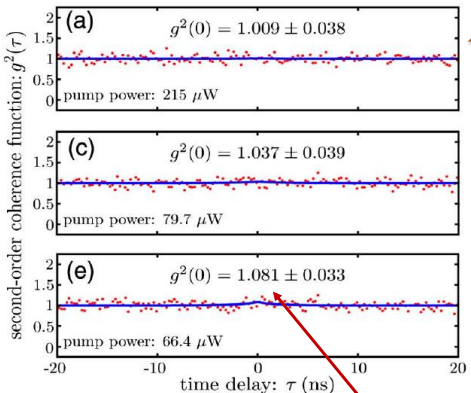
## Second-order coherence properties

W.E. Hayenga et al., Optica. 3 1187 (2016)



$$g^{(2)}(0) = 1 \text{ coherent}$$

$$g^{(2)}(0) \geq 1 \text{ chaotic}$$

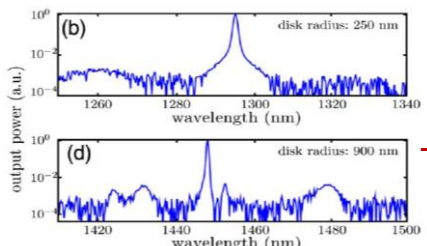
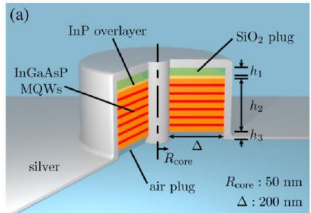


The transition from chaotic to coherent is quite gradual.

# Metallic nanolasers

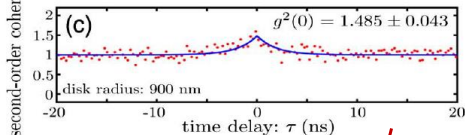
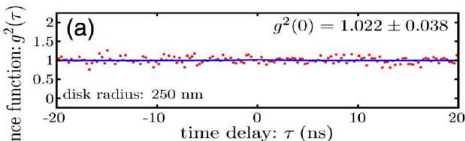
## Second-order coherence properties

W.E. Hayenga et al., Optica. 3 1187 (2016)



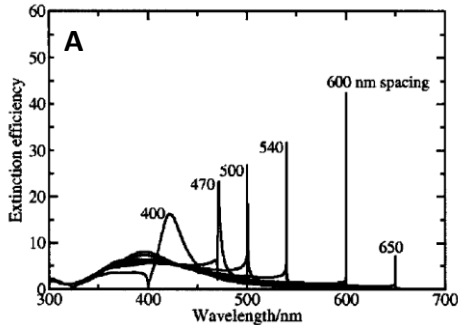
$$g^{(2)}(0) = 1 \text{ coherent}$$

$$g^{(2)}(0) \geq 1 \text{ chaotic}$$



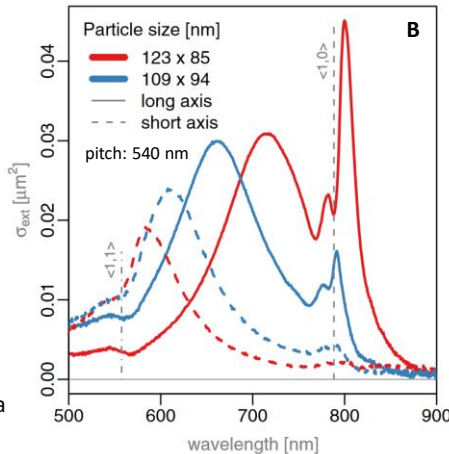
→ The disk resonator with a radius of a 900 nm supports several competing modes: the simultaneous presence of multiple modes can cause the emission to become more chaotic.

## Theory

S. Zou, N. Janel and G.C. Schatz, J. Phys. Chem. C **120** 10871 (2004)**A:** Infinite 1D chain of 50 nm Ag NPs

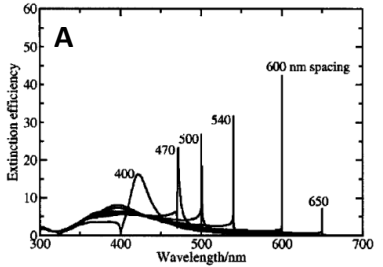
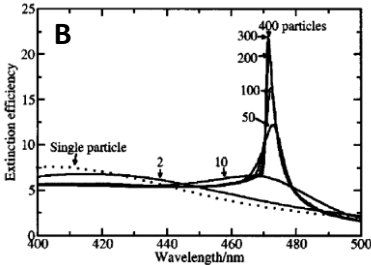
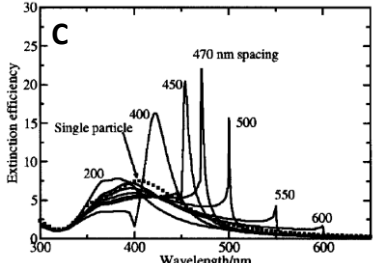
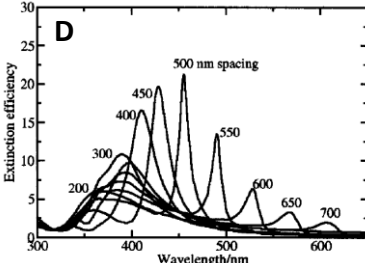
**Lattice plasmons:** hybrid modes from coupling of LSPs of individual NPs to diffractive modes in a periodic array.

## Experiment

B. Auguie, W.L. Barnes Phys. Rev. Lett. **101** 143902 (2008)**B:** 2D squared Au nanorods array

Lattice plasmons support modes with ultra-narrow line widths (< 1 nm) and **large Q values**.

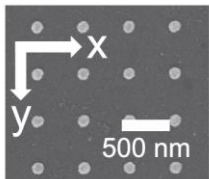
## Plasmonic nanoarrays

**A:** Infinite 1D chain of 50 nm Ag NPs**B:** 1D chain: spacing 470 nm; chain size 10-400 NPs**C:** 1D chain of 400 NPs**D:** 2D hexagonal array of 400 NPs

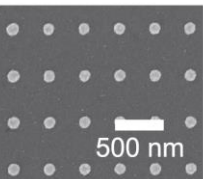
## Plasmonic surface lattice resonances on arrays of different lattice symmetries

A.D. Humphrey, W.L. Barnes, Phys. Rev. B 90 075404 (2014)

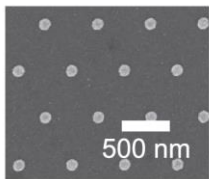
Ag nanodisks ( $d = 120 \text{ nm}$ ,  $h = 30 \text{ nm}$ )



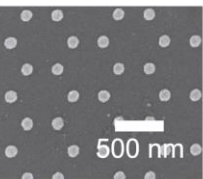
(a) Square lattice



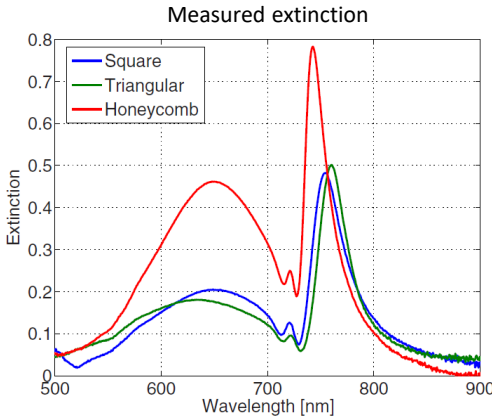
(b) Rectangular lattice



(c) Hexagonal lattice



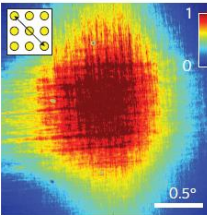
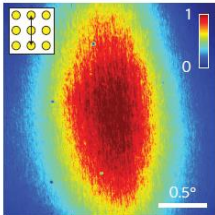
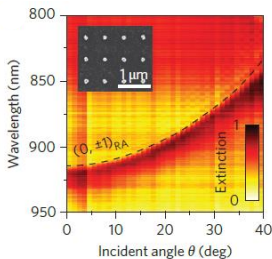
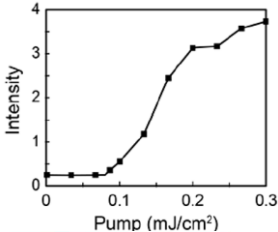
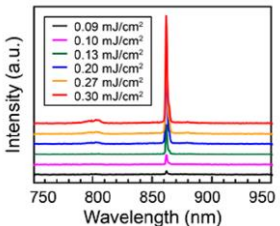
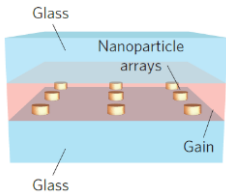
(d) Honeycomb lattice



## Plasmonic array nanolasers

Plasmonic nanoarrays support **directional lasing emission** and **efficient out-coupling** due to **constructive interference** between adjacent units.

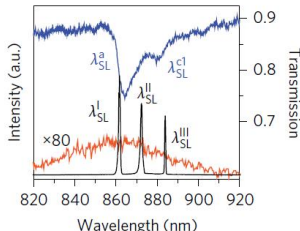
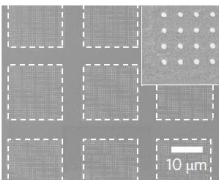
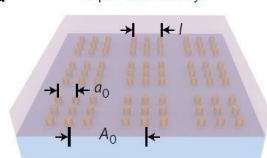
W. Zhou, ..., G. C. Schatz and T. W. Odom, "Lasing action in strongly coupled plasmonic nanocavity arrays"  
Nat. Nanotechnology **8** 506 (2013)



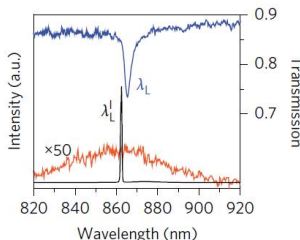
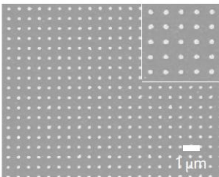
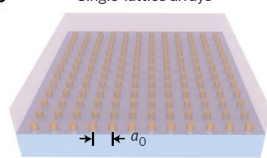
Plasmonic superlattices support **multiple band-edge modes** capable of **multi-modal nanolasing** with **large mode spacings**

D. Wang,..., G. C. Schatz and T. W. Odom, "Band-edge engineering for controlled multi-modal nanolasing in plasmonic superlattices" Nat. Nanotechnology **12** 889 (2017)

a Superlattice arrays



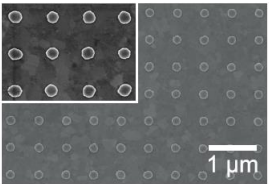
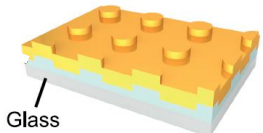
b Single-lattice arrays



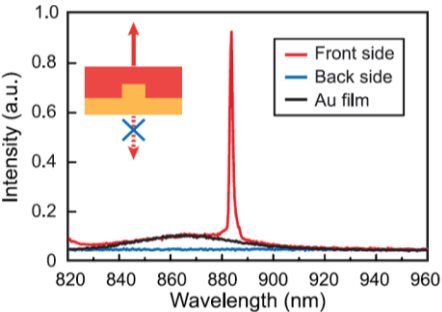
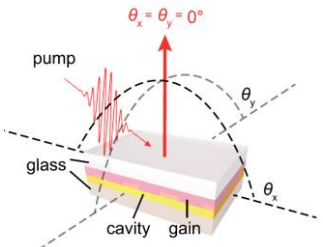
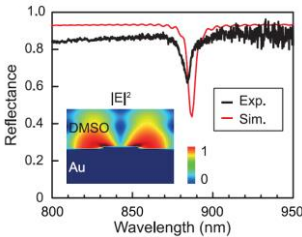
## Plasmonic array nanolasers

## Unidirectional emission

Au plasmonic crystals

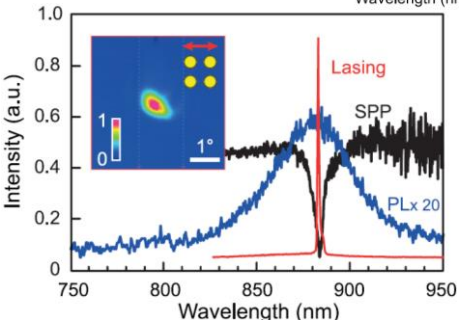
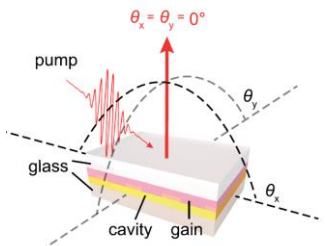
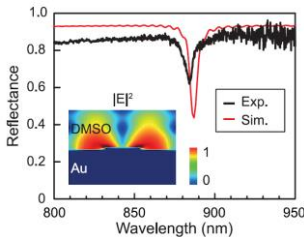
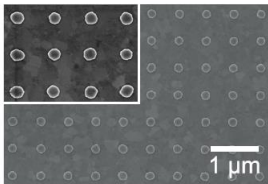
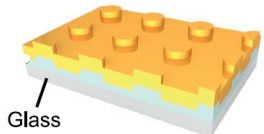


A. Yang,..., T. W. Odom, "Unidirectional Lasing from Template-Stripped Two-Dimensional Plasmonic Crystals" ACS Nano 9 11582 (2015)



## Unidirectional emission

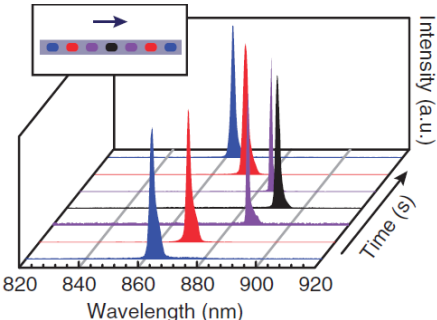
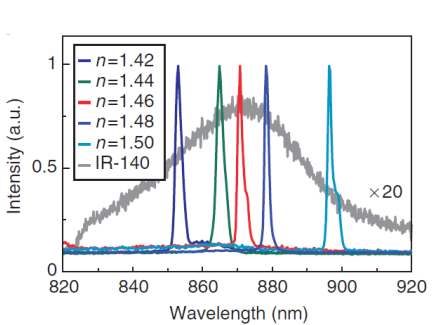
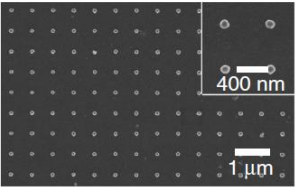
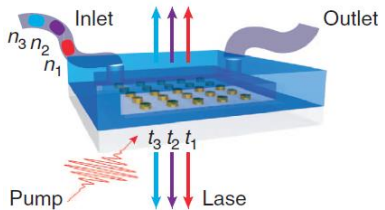
Au plasmonic crystals



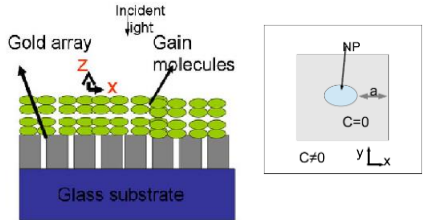
## Plasmonic array nanolasers

## Real-time tunable lasing

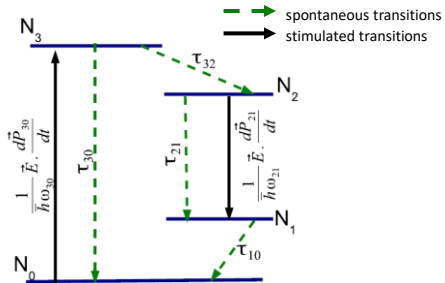
A. Yang, ..., T. W. Odom, "Real-time tunable lasing from plasmonic nanocavity arrays" Nat. Commun. 6 6939 (2015)



## Model for describing plasmon-enhanced lasers

M. Dridi and G. C. Schatz, J. Opt. Soc. Am. B **30** 2791 (2013)

Four-level model to describe the dye molecule

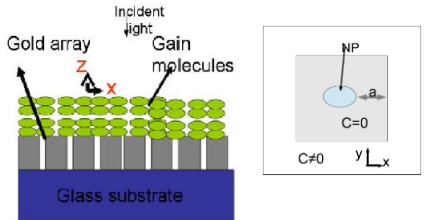


**Au nanorods** with an elliptical cross-section in a square arrangement (one per unit cell):

- major axis: 100 nm
- minor axis: 50 nm
- height: 60 nm
- grating constant: 300 nm

## Model for describing plasmon-enhanced lasers

M. Dridi and G. C. Schatz, J. Opt. Soc. Am. B **30** 2791 (2013)



$$\frac{d^2\vec{P}(t)}{dt^2} + \Delta\omega_r \frac{d\vec{P}}{dt} + \omega_r^2 \vec{P} = \kappa \Delta N(t) \vec{E}$$

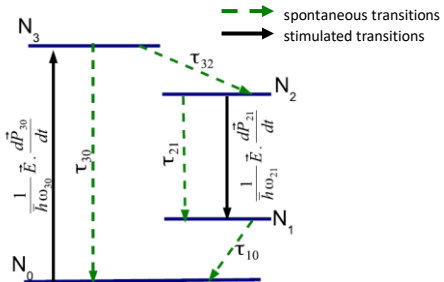
$\Delta\omega_r$  = bandwidth of the transition of interest (including radiative, nonradiative and collision effects)

$$\kappa \Delta N = \text{coupling strength} \quad \kappa = \frac{6\pi\epsilon_0 c^3 F_p \gamma_0}{\omega_r^2}$$

$F_p$  = Purcell factor

$\gamma_0$  = spontaneous decay rate

## Four-level model to describe the dye molecule

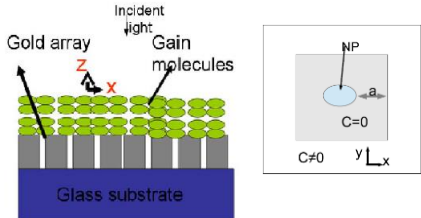


## Maxwell's equations:

$$\nabla \times \vec{E}(t) = -\mu_0 \frac{\partial \vec{H}(t)}{\partial t}$$

$$\nabla \times \vec{H}(t) = \epsilon \frac{\partial \vec{E}(t)}{\partial t} + \frac{\partial \sum_i \vec{P}_i(t)}{\partial t}.$$

## Model for describing plasmon-enhanced lasers

M. Dridi and G. C. Schatz, J. Opt. Soc. Am. B **30** 2791 (2013)

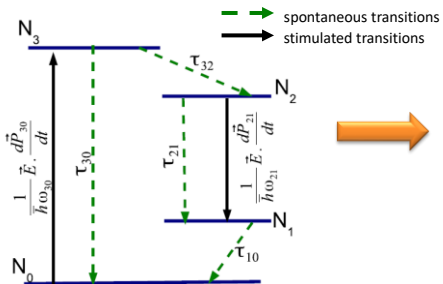
$$\frac{d^2\vec{P}(t)}{dt^2} + \Delta\omega_r \frac{d\vec{P}}{dt} + \omega_r^2 \vec{P} = \kappa \Delta N(t) \vec{E}$$

$\Delta\omega_r$  = bandwidth of the transition of interest (including radiative, nonradiative and collision effects)

$$\kappa \Delta N = \text{coupling strength} \quad \kappa = \frac{6\pi\epsilon_0 c^3 F_p \gamma_0}{\omega_r^2}$$

 $F_p$  = Purcell factor $\gamma_0$  = spontaneous decay rate

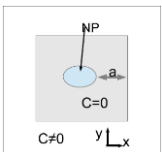
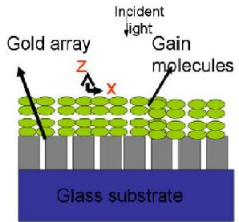
## Four-level model to describe the dye molecule



$$\left\{ \begin{array}{l} \frac{dN_3(t)}{dt} = -\frac{N_3(t)}{\tau_{32}} - \frac{N_3(t)}{\tau_{30}} + \frac{1}{\hbar\omega_{30}} \vec{E}(t) \cdot \frac{d\vec{P}_{30}(t)}{dt} \\ \frac{dN_2(t)}{dt} = \frac{N_3(t)}{\tau_{32}} - \frac{N_2(t)}{\tau_{21}} + \frac{1}{\hbar\omega_{21}} \vec{E}(t) \cdot \frac{d\vec{P}_{21}(t)}{dt} \\ \frac{dN_1(t)}{dt} = \frac{N_2(t)}{\tau_{21}} - \frac{N_1(t)}{\tau_{10}} - \frac{1}{\hbar\omega_{21}} \vec{E}(t) \cdot \frac{d\vec{P}_{21}(t)}{dt} \\ \frac{dN_0(t)}{dt} = \frac{N_1(t)}{\tau_{10}} + \frac{N_3(t)}{\tau_{30}} - \frac{1}{\hbar\omega_{30}} \vec{E}(t) \cdot \frac{d\vec{P}_{30}(t)}{dt} \end{array} \right.$$

## Plasmonic array nanolasers

## Model for describing plasmon-enhanced lasers

M. Dridi and G. C. Schatz, J. Opt. Soc. Am. B **30** 2791 (2013)

$$\frac{d^2 \vec{P}(t)}{dt^2} + \Delta\omega_r \frac{d\vec{P}}{dt} + \omega_r^2 \vec{P} = \kappa \Delta N(t) \vec{E}$$

$\Delta\omega_r$  = bandwidth of the transition of interest (including radiative, nonradiative and collision effects)

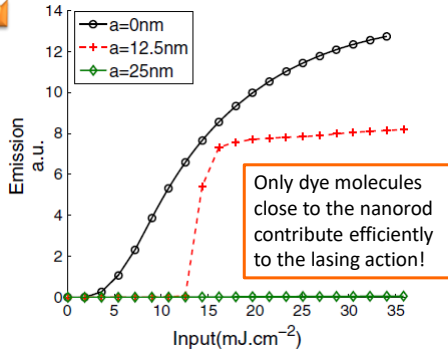
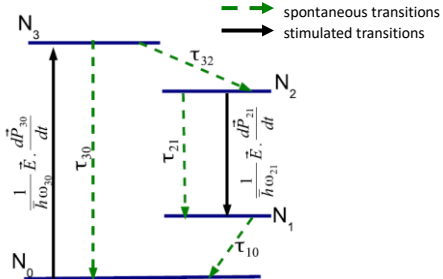
$\kappa \Delta N$  = coupling strength

$$\kappa = \frac{6\pi\epsilon_0 c^3 F_p \gamma_0}{\omega_r^2}$$

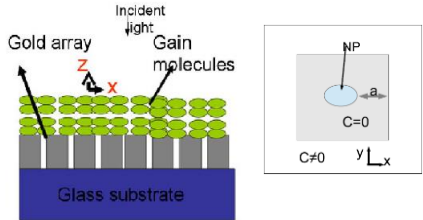
$F_p$  = Purcell factor

$\gamma_0$  = spontaneous decay rate

## Four-level model to describe the dye molecule



## Model for describing plasmon-enhanced lasers

M. Dridi and G. C. Schatz, J. Opt. Soc. Am. B **30** 2791 (2013)

$$\frac{d^2\vec{P}(t)}{dt^2} + \Delta\omega_r \frac{d\vec{P}}{dt} + \omega_r^2 \vec{P} = \kappa \Delta N(t) \vec{E}$$

$\Delta\omega_r$  = bandwidth of the transition of interest (including radiative, nonradiative and collision effects)

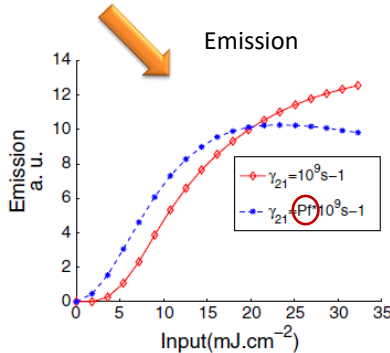
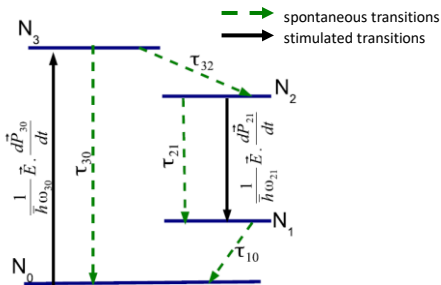
$\kappa \Delta N$  = coupling strength

$$\kappa = \frac{6\pi\epsilon_0 c^3 F_p \gamma_0}{\omega_r^2}$$

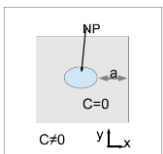
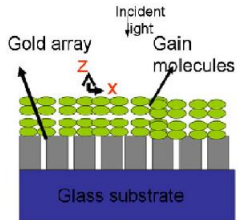
$F_p$  = Purcell factor

$\gamma_0$  = spontaneous decay rate

## Four-level model to describe the dye molecule



## Model for describing plasmon-enhanced lasers

M. Dridi and G. C. Schatz, J. Opt. Soc. Am. B **30** 2791 (2013)

$$\frac{d^2\vec{P}(t)}{dt^2} + \Delta\omega_r \frac{d\vec{P}}{dt} + \omega_r^2 \vec{P} = \kappa \Delta N(t) \vec{E}$$

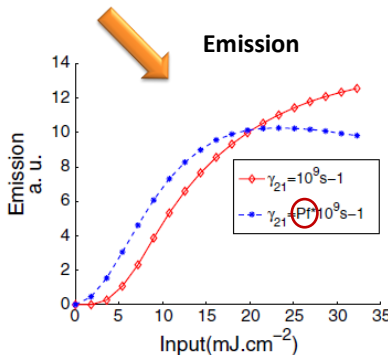
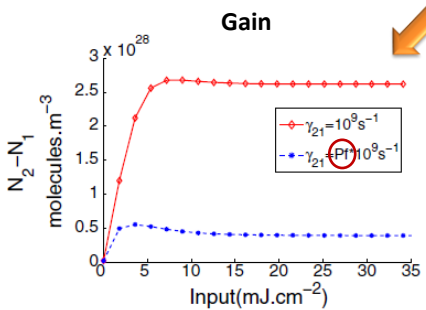
$\Delta\omega_r$  = bandwidth of the transition of interest (including radiative, nonradiative and collision effects)

$\kappa \Delta N$  = coupling strength

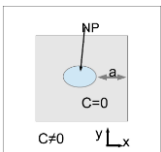
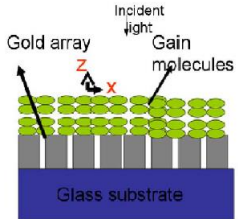
$$\kappa = \frac{6\pi\epsilon_0 c^3 F_p \gamma_0}{\omega_r^2}$$

$F_p$  = Purcell factor

$\gamma_0$  = spontaneous decay rate



## Model for describing plasmon-enhanced lasers

M. Dridi and G. C. Schatz, J. Opt. Soc. Am. B **30** 2791 (2013)

$$\frac{d^2\vec{P}(t)}{dt^2} + \Delta\omega_r \frac{d\vec{P}}{dt} + \omega_r^2 \vec{P} = \kappa \Delta N(t) \vec{E}$$

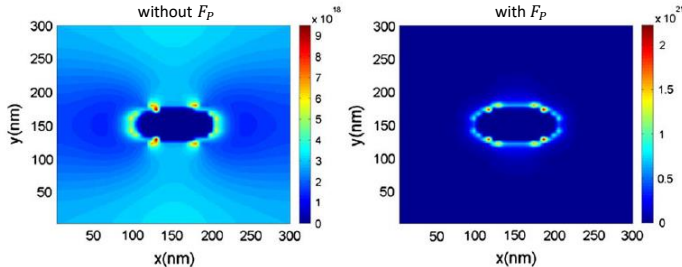
$\Delta\omega_r$  = bandwidth of the transition of interest (including radiative, nonradiative and collision effects)

$\kappa \Delta N$  = coupling strength

$$\kappa = \frac{6\pi\epsilon_0 c^3 F_p \gamma_0}{\omega_r^2}$$

$F_p$  = Purcell factor

$\gamma_0$  = spontaneous decay rate

coupling strength ( $\kappa \Delta N$ )

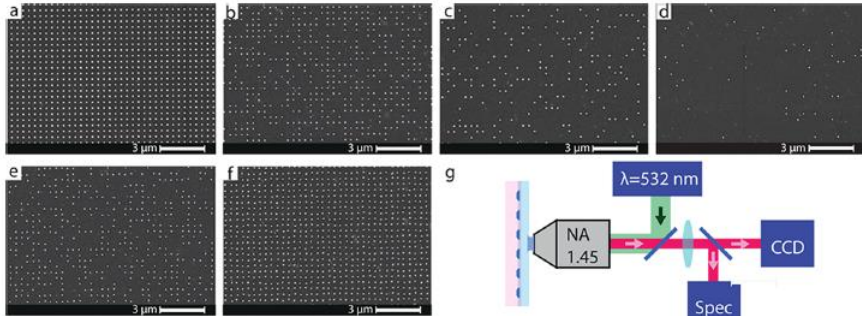
Despite the decrease of the gain, better lasing action (lower threshold, higher emission intensity) is obtained due to an increase of the coupling strength between dye and plasmon.

## Plasmonic array nanolasers

## Statistics of Randomized Plasmonic Lattice Lasers

A.H. Schokker and A.F. Koenderink, ACS Photonics 2 1289 (2015)

Square lattice of Ag NPs (diameter 50 nm, height 30 nm); interparticle distance: 380 nm



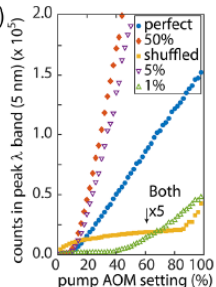
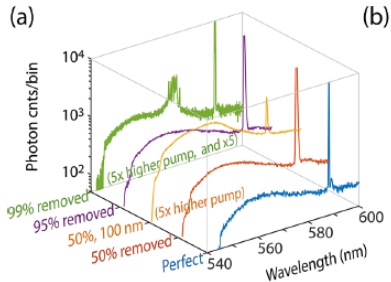
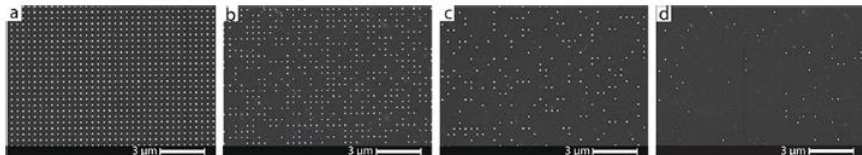
(a-d): particles randomly removed to leave fill factors of 100%, 50%, 20%, and 5%

(e, f): fill factor of 50% and 100%, with particles randomly placed in a box of 100 nm centered on each perfect-lattice site

## Statistics of Randomized Plasmonic Lattice Lasers

A.H. Schokker and A.F. Koenderink, ACS Photonics 2 1289 (2015)

Square lattice of Ag NPs (diameter 50 nm, height 30 nm); interparticle distance: 380 nm



Only for the very dilute sample (99% removed) a much larger threshold than for the other cases is found.

The perfect sample has a smaller slope above the threshold, indicating poorer outcoupling.